# Soft-x-ray emission and inelastic electron-scattering study of the electronic excitations in amorphous and crystalline silicon dioxide

V. Jeyasingh Nithianandam and S. E. Schnatterly
*Jesse Beams Laboratory of Physics, University of Virginia, Charlottesville, Virginia 22901*
(Received 7 March 1988)

The valence-band electronic structures of amorphous and crystalline $SiO_2$ are examined with soft-x-ray emission spectroscopy. In addition, the absorption spectra of $a$-$SiO_2$ obtained by inelastic electron scattering (IES) near the interband threshold and Si $L_{23}$ threshold regions are presented. Simple models used to describe the absorption in these spectral regions give consistent values for the size of the band gap of $SiO_2$. An empirical model based on these results is presented to explain the positions of peaks in the ultraviolet optical spectrum and the IES valence excitation spectrum of $SiO_2$. The Si $2p$ core exciton observed in both x-ray emission and absorption spectra is discussed.

## INTRODUCTION

Soft-x-ray emission spectroscopy (SXES) provides basic information about the valence-band electronic structure of solids. Inelastic-electron-scattering (IES) measurements have been used to study interband transitions and absorption near core thresholds. We present here the Si $L_{23}$ x-ray valence-band emission spectrum and IES spectra of silicon dioxide in the energy range of the Si $L_{23}$ edge and in the energy range of valence- to conduction-band transitions.

The optical-absorption spectrum of silicon dioxide in the valence range remains one of the major unsolved problems in the optical spectra of solids.[1] There is even a significant uncertainty in the size of the band gap for this material. One of the purposes of the present work is to provide new information about the size of the band gap of silicon dioxide obtained by describing these spectroscopic data near threshold with simple models.

## PRINCIPLE AND EXPERIMENTAL DETAILS

The descriptions of our SXE and IES spectrometers are given elsewhere.[2,3] The SXE spectra were excited by bombardment of the sample with an electron beam of 1–3 keV energy. The soft-x-ray photons emitted due to electronic transitions from occupied valence or conduction states to the vacancy in the Si $2p$ core level were energy dispersed by a toroidal grating and detected by a position-sensitive photodiode array detector. The energy resolution of our SXE spectrometer in this energy range is about 0.1 eV. The sample was a 3000-Å-thick film of amorphous silicon dioxide on a $c$-Si substrate. The film was grown by a chemical-vapor-deposition (CVD) process and is nearly stoichiometric. We also present x-ray emission spectra from a crystalline quartz sample. The quartz sample was "heat sunk" very well using a special mount on a sample holder, and the temperature of the sample was about 120 K during electron-beam excitation. The incident-electron beam spot of about $1\times0.5$ mm$^2$ size was changed to a new location on the $SiO_2$ sample every 5 min to prevent electron-beam-induced decomposition of the sample. This was repeated several times over a period of several hours and the SXE spectra reported here are nearly free of electron-beam-induced decomposition. In the IES measurements a monoenergetic beam of 300-keV electrons was passed through an evaporated amorphous silicon dioxide thin film 500 Å thick, and the transmitted intensity was recorded as a function of energy loss with a resolution of 0.14 eV.

## DATA REDUCTION

Data processing of our raw $L$ x-ray emission spectra of silicon dioxide samples includes removal of unwanted multiple-order oxygen $K$ emission contributions, and $E^3$ division and normalization of spectra to an area of unity as reported in our earlier work.[4] The $L$ x-ray emission spectra if $SiO_2$ obtained with 1.5- and 3-kV incident-electron energies line up in the energy regions below 70 eV and above 110 eV, and the shape of these two spectra between 70 and 110 eV agree well. The effects of self-absorption in the x-ray emission spectra presented here are negligible and do not alter any of our conclusions.

## VALENCE-BAND X-RAY EMISSION

The Si $L_{23}$ valence-band emission spectra obtained using a 1.5-kV electron-beam excitation from amorphous and crystalline silicon dioxide are shown in Figs. 1 and 2, respectively. We found that quartz was more susceptible to electron-beam-induced damage than $a$-$SiO_2$, and hence the SXE spectrum in Fig. 1 has better statistics than the spectrum in Fig. 2. The x-ray emission spectrum of $SiO_2$ contains a series of peaks, so using a spectral synthesis method described in detail in our earlier work,[4] we fitted these spectra with a small number of line-shape functions. In general, line shapes in x-ray spectra are influenced by lifetime broadening of the valence and core hole, phonon coupling, disorder in the sample, and the effects of the instrument. A Lorentzian distribution function accounts for the lifetime broadening of the valence and core hole.[5] The broadening due to phonon coupling,

 

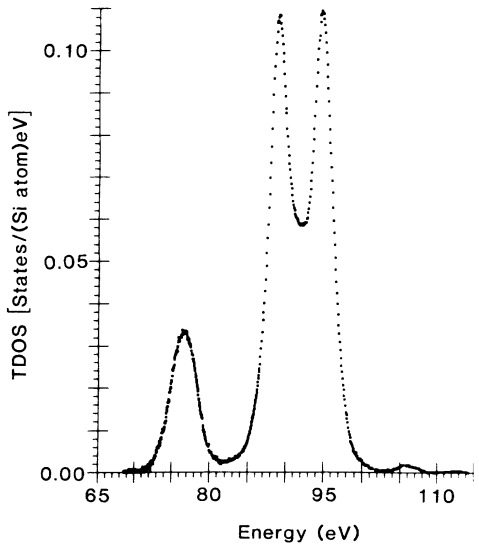


FIG. 1. Si $L$ x-ray emission band from amorphous silicon dioxide. The area under the emission band has been normalized to unity.

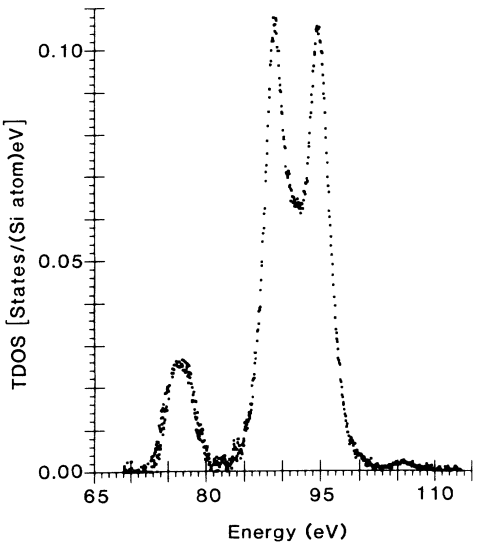


FIG. 2. Si $L$ x-ray emission band from crystalline quartz.

effects of the instrument, and disorder could be represented by a Gaussian function.[5] Therefore we assumed a Voigt profile for our line shape.[6] The Voigt profile results from the convolution of a Lorentzian and a Gaussian line shape, and so it accounts well for the Lorentzian and Gaussian contributions to the broadening due to the different mechanisms that affect the line shapes in our x-ray spectra.

We used the smallest number of Voigt components of reasonable full width at half maximum (FWHM) that could produce a good fit to each valence-band x-ray emission spectrum. The parameters in the nonlinear least-squares program were allowed to vary freely. The root-mean-square deviation of the fits from the data is 1% of the peak intensity. The description of the parameters and their values obtained from these fits are given in Table I. The energy positions of the peaks are accurate to within $\pm 0.05$ eV, and the amplitudes of these peaks are good to about 2% of their values. The positions of these peaks agree well with the features in valence-band XPS data on $SiO_2$ (Ref. 7) and may correspond to calculated molecular orbital energies,[8] as discussed later. These parameters will allow others to reproduce our data in a convenient and accurate manner. Figure 3 shows a fit to the $L$ x-ray emission spectrum of $a$-$SiO_2$ using this method.

Various calculations of the electronic density-of-states distribution of $SiO_2$, XPS, and SXES measurements have been reported.[7–18] The molecular-orbital calculations of Tossell[8] on a $SiO_4^{4-}$ cluster representing $SiO_2$ yields seven molecular-orbital energy levels. The lower valence subband from 70–85 eV has predominantly O 2$s$ character with some hybridization with Si 3$s$ and 3$p$ states.[9] The peak centered at about 95 eV in the upper valence subband has been attributed to nonbonding oxygen 2$p$ or-

TABLE I. Parameters of the multipeak fit to the valence-band emission spectra of $a$-$SiO_2$ and quartz. $E_i$ is the energy position of the peak. $\Gamma_G$ and $\Gamma_L$ are the full widths at half maximum (FWHM) of the Gaussian and Lorentzian parts of the Voigt profile in eV. $N(E_i)$ is the intensity at the peak in transition–density-of-states (TDOS) units and $A(E_i)$ is the area of the peak in units of states/Si.

| | Peaks | | | | | |
|---|---|---|---|---|---|---|
| Parameter | $A$ | $B$ | $C$ | $D$ | $E$ | $F$ |
| | | | Amorphous silicon dioxide | | | |
| $E_i$ | 74.87 | 76.79 | 88.92 | 91.97 | 94.43 | 95.78 |
| $\Gamma_G$ | 3.38 | 3.65 | 2.17 | 2.68 | 2.08 | 2.55 |
| $\Gamma_L$ | 0.07 | 0.01 | 1.45 | 0.00 | 0.43 | 0.83 |
| $N(E_i)$ | 0.006 | 0.030 | 0.103 | 0.037 | 0.078 | 0.039 |
| $A(E_i)$ | 0.021 | 0.12 | 0.40 | 0.11 | 0.20 | 0.12 |
| | | | Quartz | | | |
| $E_i$ | 75.17 | 76.96 | 88.85 | 91.77 | 94.47 | 95.59 |
| $\Gamma_G$ | 1.28 | 2.93 | 1.69 | 2.34 | 1.76 | 2.19 |
| $\Gamma_L$ | 2.36 | 0.31 | 2.08 | 2.66 | 0.85 | 1.45 |
| $N(E_i)$ | 0.010 | 0.021 | 0.080 | 0.036 | 0.063 | 0.038 |
| $A(E_i)$ | 0.043 | 0.073 | 0.36 | 0.20 | 0.17 | 0.14 |

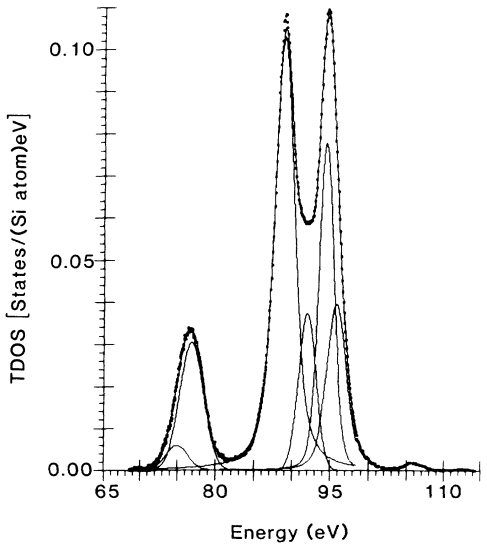


FIG. 3. Fit to the valence-band x-ray emission spectrum of $a$-$SiO_2$ with six broadened line-shape functions.

bitals.[9] The emission near the bottom of the upper valence subband is due to bonding orbitals involving oxygen $2p$ and $2s$ states and $3p$ or $3s$ silicon states.

The effects of disorder on the DOS can be seen by comparing the SXE spectra of $a$-$SiO_2$ and quartz. The valley at about 92 eV in our valence-band x-ray emission spectrum is deeper for $a$-$SiO_2$ than quartz. Moreover, we find from Table I that the width and the area of the peak at about 92 eV are smaller for $a$-$SiO_2$ than quartz. Laughlin *et al.*[9] compared the tight-binding DOS for quartz and the cluster-Bethe-lattice DOS of $a$-$SiO_2$. They show that the peak 6 eV below the valence-band maximum in their DOS is narrower in $a$-$SiO_2$ than quartz. It is unusual for a DOS structure to be sharper in an amorphous material than a corresponding crystalline phase, as has been predicted and observed here.

The electron-energy-loss spectroscopy (EELS) measurements of $a$-$SiO_2$ by Ibach and Rowe[19] showed that the top of the valence band lies 10.6 eV below the vacuum level. In our SXE spectra the position of the top of the valence band of both $a$-$SiO_2$ and quartz is at 97.5 eV ($L_3$). Combining these two results with an electron-affinity value of 0.9 eV (Ref. 20) allows us to obtain the energy positions of the Voigt components below the vacuum level. These values are shown in Table II. There is a good agreement of these energy positions with the molecular-orbital energies of quartz obtained from the positions of structures in the XPS spectrum[7] and a moderate agreement with molecular-orbital calculations.[7,8] In calculations based on molecular-orbital cluster models, the lattice is ignored, and the accuracy of the results strongly depend upon the size of the cluster. Therefore we only use the calculated ordering of the molecular orbitals to assign identities to the peaks in our fit to the spectrum.

## X-RAY EMISSION NEAR THE VALENCE-BAND EDGE AND IN THE GAP REGION

We developed a nonlinear least-squares program to fit the measured spectra of silicon dioxide in the region 95.2–110 eV, which includes the top of the valence band, the band-gap region, and the bottom of the conduction band. This model is described in detail in our previous work.[4] We briefly outline it here. We use a straight line $A_t(E_t - E)$ convoluted with a Gaussian broadening function of FWHM $\Gamma$ to fit the top of the $L_{23}$ valence-band emission spectrum. $E_t$ is the position of the top of the valence band, and $A_t$ is a constant. We call the resulting function $V(E)$. We used an exponential energy-band tail[21,22] convoluted with a Gaussian broadening function for the shape of the DOS near the valence-band edge of amorphous silicon dioxide, and this function $T(E)$ is joined to the function $V(E)$ so as to best fit the data.

The emission near the conduction-band minimum or the $L_{23}$ x-ray absorption edge is due to the Si $2p$ core exciton. We used in our fit a Voigt line-shape function for the core exciton. Thus our model for $a$-$SiO_2$ in the gap region includes $V(E)$, $T(E)$, and Voigt functions for the core exciton. The Voigt function at the higher-energy position in the fit to $a$-$SiO_2$ spectrum represents the rest of the exciton series and/or conduction-band states. The value of the $L_3$ valence-band maximum position for $a$-$SiO_2$ obtained from the fit to the data agrees reasonably well with the value of 98.0 eV obtained for the valence-band maximum of $a$-$SiO_2$ by the extrapolation of the steepest descent of the leading edge of the valence-band spectrum. A fit based on this model to the spectrum of $a$-$SiO_2$ for states at the top of the valence band and in the gap region is shown in Fig. 4.

We compared several $L$ x-ray emission spectra of $c$-$SiO_2$ and amorphous silicon in the region 99–102 eV and

TABLE II. Energy positions of molecular orbitals of $SiO_2$ obtained from SXES and XPS spectra (Ref. 7) and Tossell's calculations (Ref. 8).

| | | Position of features below vacuum level | | | |
|---|---|---|---|---|---|
| Peak | Molecular orbital | Tossell | SXE $a$-$SiO_2$ | SXE quartz | XPS quartz |
| $A$ | $4A_1$ | 29.33 | 33.18 | 33.05 | 31.50 |
| $B$ | $3T_2$ | 26.66 | 31.26 | 31.26 | 30.30 |
| $C$ | $5A_1$ | 19.45 | 19.13 | 19.37 | 19.45 |
| $D$ | $4T_2$ | 15.33 | 16.08 | 16.45 | 16.75 |
| $E$ | $1E$ | 13.66 | 13.62 | 13.75 | 13.45 |
| $F$ | $5T_2$,$1T_1$ | 13.0, 12.66 | 12.28 | 12.62 | 11.95 |

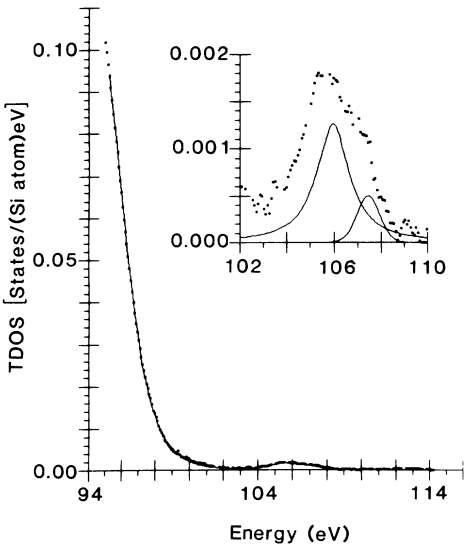


FIG. 4. The valence-band edge and gap region part of the $L$ x-ray emission spectrum of $a$-$SiO_2$ and fit based on model described in the text. The inset is an enlargement of the emission near the conduction-band edge.

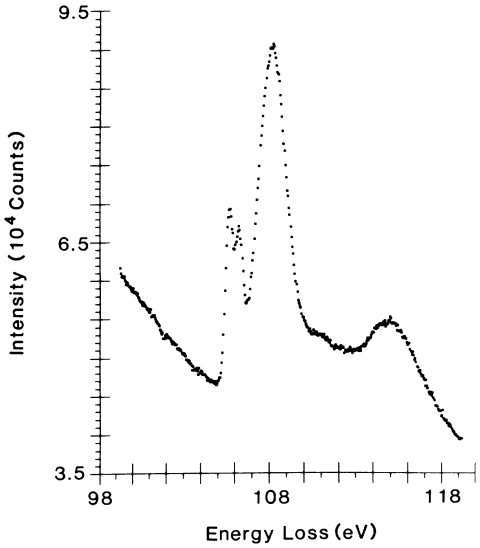


FIG. 5. Loss function of $a$-$SiO_2$ in the energy range of the Si $L_{23}$ edge obtained by inelastic-electron-scattering spectroscopy for small momentum transfer.

observed unexpected extra strength in the spectrum of $c$-$SiO_2$. This is apparently due to a small amount of electron-beam-induced damage associated with excess Si inside or on the surface of $c$-$SiO_2$. The fitting program takes these states into account by the function $T(E)$. The values of the parameters of these fits to our data are shown in Table III.

## INTERPRETATION OF IES SPECTRA

The absorption spectrum of evaporated $a$-$SiO_2$ near the Si $L_{23}$ threshold is shown in Fig. 5. The shape of this spectrum is in agreement with previous measurements.[23] We developed a simple Frenkel model for the shape of the absorption data in the threshold region. The model includes a step function convoluted with a Gaussian for the continuum absorption as is done with an Elliot model[24] and a Gaussian peak for the Si $2p$ core exciton. The spin-orbit splitting and intensity of the two components were adjustable parameters in our program. We obtained 0.58 eV and 0.8 for spin-orbit splitting and branching ratio, respectively. The absorption edge of $a$-$SiO_2$ ($L_3$) was found to be at 107.1 eV, and the corresponding Si $2p$ core exciton was found to be at 105.67 eV. The values of parameters of the fit to the $a$-$SiO_2$ data are shown in Table IV. Figure 6 shows a fit to the data. Using the value of 97.5 eV for the top of the valence band ($L_3$) of both $a$-$SiO_2$ and quartz with the $L_3$ continuum threshold of 107.1 eV, we obtain a value of 9.6 eV for the band gap of silicon dioxide.

Kotani and Toyozawa argue that the branching ratio of exciton states could deviate from its statistical value due to mixing of spin-orbit partners by the electron-hole exchange interaction.[25] In $SiO_2$ we obtain a branching ratio of 0.8 for the Si $2p$ core exciton in the absorption spectrum. This deviation from the statistical value of 0.5 may be due to the Kotani-Toyozawa mechanism. In passing we note that the spin-orbit-splitting value of 0.58 eV for $SiO_2$ is slightly lower than the value of 0.61 eV ob-

TABLE III. Model parameters for the top of the valence band and gap region of $SiO_2$. $E_t$ is the position of the top of the valence band in eV. $A_t$ is the slope of the function representing the top of the valence band in units of states/eV$^2$ Si-atom. $\Gamma$ is the FWHM of the Gaussian broadening function in eV. $M$ is the energy position at which the $T(E)$ function joins the $V(E)$ function, and $W$ is the width of the exponential energy band tail in eV. $N_t$ is the number of states/Si-atom at $M$. $\Gamma_{v1}$ and $\Gamma_{v2}$ are the FWHM of the Voigt functions in eV.

| | Parameters | | | | | | |
|---|---|---|---|---|---|---|---|
| Sample | $E_t$ | $A_t$ | $\Gamma$ | $M$ | $W$ | $N_t$ | |
| $a$-$SiO_2$ | 97.45 | $1.33\times10^{-3}$ | 1.84 | 96.78 | 1.1 | $4.9\times10^{-3}$ | |
| Quartz | 97.51 | $1.13\times10^{-3}$ | 2.09 | 96.69 | 1.25 | $5.4\times10^{-3}$ | |
| | $E_1$ | $\Gamma_{v1}$ | $N(E_1)$ | $E_2$ | $\Gamma_{v2}$ | $N(E_2)$ | $\chi^2$ |
| $a$-$SiO_2$ | 105.32 | 1.64 | $1.2\times10^{-3}$ | 106.82 | 1.13 | $5\times10^{-4}$ | 3.4 |
| Quartz | 105.60 | 3.92 | $1.2\times10^{-3}$ | | | | 2.0 |

TABLE IV. Parameters of the Frenkel-model fit to the IES spectrum in the energy range of the Si $L_{23}$ edge. $E_e$ is the position of the exciton and $\Gamma_e$ is the FWHM of the Gaussian function representing the exciton in eV. $E_{\rm th}$ is the position of the $L_3$ absorption threshold and $\Gamma_B$ is the FWHM of the broadening function in eV. $S$ is the spin-orbit splitting and $R$ the branching ratio.

| $E_e$ | $\Gamma_e$ | $E_{\rm th}$ | $\Gamma_B$ | $S$ | $R$ | $\chi^2$ |
|---|---|---|---|---|---|---|
| 105.67 | 0.53 | 107.05 | 1.26 | 0.58 | 0.8 | 1.2 |

tained from absorption measurements of Si in our laboratory and others'.[26] This difference is small but may be real.

The IES spectra from $a$-$SiO_2$ for a momentum transfer $q \simeq 0$ in the region of interband transitions is shown in Fig. 7. The features at about 10.6, 12.5, 14.5, and 17.8 eV in Fig. 6 are in agreement with reported EELS measurements obtained in reflection.[27–29] Laughlin[30] carried out a detailed study of the optical-absorption spectrum of $SiO_2$. According to his calculations, there is a forbidden valence exciton at 8.4 eV, and the peak at about 10.6 eV in Fig. 7 is due to an excitonic resonance superimposed on a background of interband transitions. The lack of temperature dependence of the width of this peak is consistent with this interpretation.[31] According to calculations,[9] the highest valence-band states of $SiO_2$ are derived from the nonbonding O $2p$ orbitals. The lowest conduction states are formed from a linear combination of $s$ functions on oxygen and silicon atoms, all with the same phase.[9,15] The relative phases of the O $2p$ orbitals in the valence-band wave functions cause the electric dipole transition matrix elements between the highest valence-band states and the lowest conduction-band states to be zero.[15] We expect, therefore, to see an interband absorption spectrum starting with zero strength at threshold and increasing uniformly with energy. Visual inspection

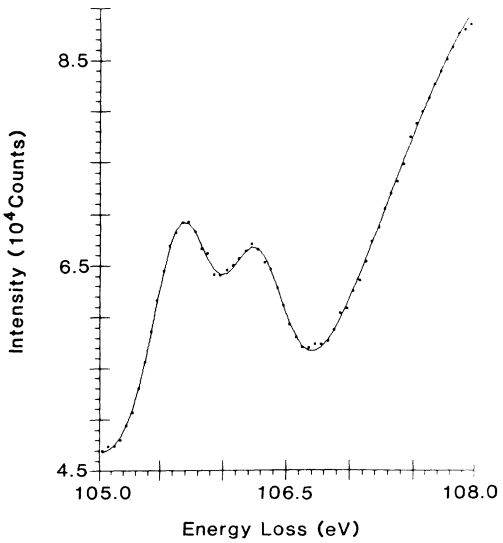


FIG. 6. Frenkel model fit to the IES spectrum of $a$-$SiO_2$ near the Si $L_{23}$ threshold.

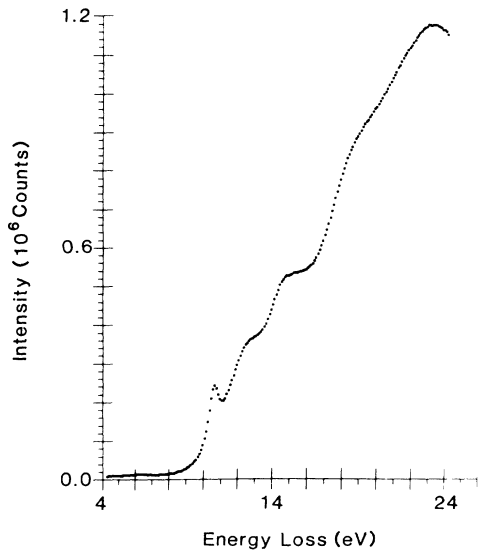


FIG. 7. Loss function of $a$-$SiO_2$ due to valence- to conduction-band transitions obtained by inelastic electron scattering.

of the IES data in Fig. 7 well above the band gap suggests a straight line shape for the continuum absorption. Accordingly, we fit the region 6–12.3 eV in the data in Fig. 7 with a convolution of a linear function $B(E-E_g)$ with a Gaussian, a constant for the background, and a Gaussian function for the excitonically enhanced peak at about 10.6 eV. $E_g$ is the value of the band gap and $B$ is a constant. The fit to the data is shown in Fig. 8. The fit parameters are shown in Table V. The value of 9.7 eV for the band gap of $a$-$SiO_2$ obtained from the fit to the IES valence excitation spectrum is in excellent agreement with the value of 9.6 eV obtained from the position of the valence-band maximum in our SXE spectra and $L_3$ continuum absorption threshold of $SiO_2$ in our IES spectrum.

Weinberg *et al.*[32] have reviewed other experimental determinations of the band gap of $SiO_2$ and report a value of 9.3 eV for the band gap of $SiO_2$ from photoconductivity measurements. We have obtained consistent values for the band gap of $a$-$SiO_2$ by analyzing two different spectral regions of our IES data, namely interband absorption threshold and Si $L_{23}$ absorption threshold regions with simple models, and this lends credence to the simple models we used to describe our data. Both SXES and IES measurements give bulk value for the band gap of $SiO_2$, and so surface or impurity effects are negligible in our estimation of the size of the band gap of $SiO_2$. Sta-

TABLE V. Parameters of the fit to the IES spectrum in the energy range of the fundamental interband threshold. $E_g$ is the value of the band gap and $\Gamma_G$ is the FWHM of the Gaussian broadening function in eV. $E_{\rm ER}$ is the position and $\Gamma_{\rm ER}$ is the FWHM of the Gaussian representing the exciton resonance peak.

| $E_g$ | $\Gamma_G$ | $E_{\rm ER}$ | $\Gamma_{\rm ER}$ | $\chi^2$ |
|---|---|---|---|---|
| 9.73 | 2.33 | 10.59 | 0.63 | 27.6 |

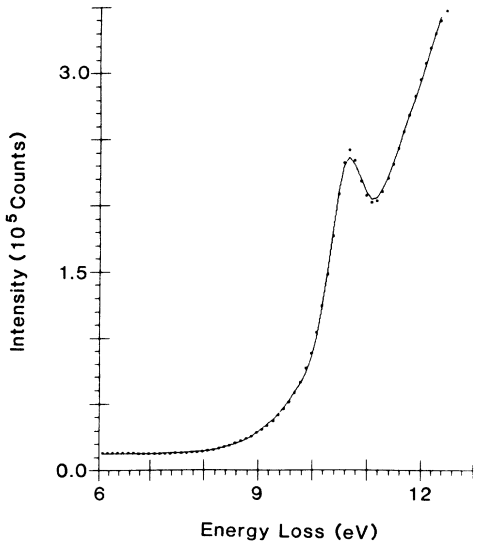


FIG. 8. IES spectrum of $a$-$SiO_2$ for a momentum transfer $q \simeq 0$ in the region of the interband threshold and a fit to the data based on the model described in the text.

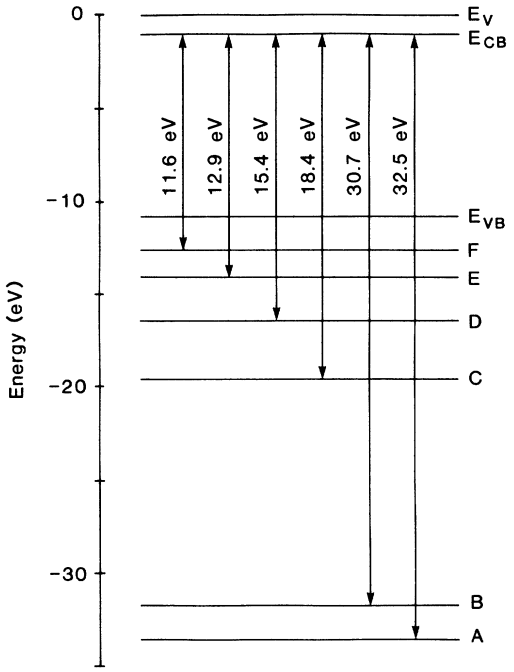


FIG. 9. Schematic diagram of molecular-orbital energy levels obtained from the $L_{23}$ valence-band x-ray emission spectrum and the valence absorption spectrum of $a$-$SiO_2$. $A$–$F$ refer to the valence energy components shown in Tables I and II. $E_V$, $E_{CB}$, and $E_{VB}$ represent vacuum level, conduction-band edge, and valence-band edge, respectively. Vertical arrows indicate the energy difference between the conduction-band bottom and a given molecular orbital.

tistical and other uncertainties in our estimation of the band gap of $SiO_2$ are about 0.1 eV and are within limits of the energy resolutions of SXE and IES spectrometers.

Phillip first carried out reflectivity measurements on $a$-$SiO_2$ and crystalline quartz.[33] He observed four prominent peaks between 10 and 18 eV in the spectrum. By means of a Kramers-Kronig analysis of our IES spectrum, we have evaluated the real and imaginary parts of the dielectric function and the optical reflectivity of $a$-$SiO_2$, finding good agreement with Phillip's results. According to Laughlin[30] these four prominent peaks in the optical reflectivity spectra of $SiO_2$ are excitonic resonances due to transitions from the nonbonding and bonding states in the upper valence subband of $SiO_2$. The energy differences between the four Voigt components of the upper valence subband of $SiO_2$ obtained from the fit to our $L$ x-ray emission spectrum agree reasonably well with the corresponding differences between the energy positions of the peaks in the reflectivity spectrum. It is tempting to speculate, therefore, that the features in the reflectivity spectra are due to transitions from upper valence-subband molecular orbitals to the same final state.[7] Using the information obtained from the SXES and IES measurements, we constructed a model similar to a model based on XPS data[19,34] for the experimentally observed electron-energy levels and transitions for $a$-$SiO_2$ shown in Fig. 9. According to this model, the four peaks in the reflectivity and IES spectra are due to excitons involving the molecular orbitals of the upper valence subband of $SiO_2$, and in each case the exciton binding energy is about 1.2 eV. We used in this model the positions of the Voigt components of the multipeak fit to the valence-band x-ray emission spectrum. Table VI shows the different energy values of the transitions we propose to explain the features in the optical reflectivity and IES spectra. This empirical model is very simple, and so further calculations will be necessary to confirm it.

TABLE VI. Comparison of energy values of transitions from different molecular orbitals of the valence band to states at the conduction-band minimum and positions of peaks in the optical reflectivity spectrum. $E_{MO}$ is the difference between the position of the Voigt components of the valence-band TDOS and the valence-band maximum. The column labeled $R(E)$ shows the energies of the peaks in the reflectivity spectrum. These energies are similar to, but not the same as, those of the corresponding features in the IES spectrum. $E_g$ is the band gap of $a$-$SiO_2$ obtained from the fit to the IES spectrum in Fig. 8. $E_B$ is the estimated binding energy of excitons observed in Fig. 7 above the interband absorption threshold. The energy of transitions from peaks $A$ and $B$ of the lower valence subband correspond to peaks at 28.2 and 31.0 eV in other EELS data (Refs. 28 and 29).

| Peak | $E_{MO}$ | $E_{MO}+E_g$ | $R(E)$ | $E_B=E_{MO}+E_g-R(E)$ |
|---|---|---|---|---|
| $F$ | 1.88 | 11.58 | 10.3 | 1.28 |
| $E$ | 3.22 | 12.92 | 11.7 | 1.22 |
| $D$ | 5.69 | 15.39 | 14.3 | 1.09 |
| $C$ | 8.74 | 18.44 | 17.3 | 1.14 |
| $B$ | 20.87 | 30.69 | | |
| $A$ | 22.78 | 32.48 | | |

The fit to the Si $2p$ core-exciton peak at 105.7 eV in the $L_{23}$ absorption spectrum yields a Gaussian standard deviation $\sigma$ of 0.2 eV for the width. If the transition from the $2p$ core level to the bottom of the conduction band is coupled linearly to phonons of frequency $\omega$, the absorption will be broadened in a Gaussian shape with a standard deviation $\sigma$ given by

$$\sigma^2 = S(\hbar\omega)^2 \coth(\hbar\omega/2kT) ,$$

where $S$ is a dimensionless coupling constant equal to the mean number of phonons created in the transition.[35] For this highly localized core transition, the most important modes are likely to be longitudinal-optical phonons with $\hbar\omega_{LO}=0.153$ eV.[36,37] Using our absorption value for $\sigma$ and $T=300$ K, we find $S=2.0$. According to the linear coupling model[38] the excited state relaxes to a new configuration after absorption occurs by radiating the phonons which have been created to the rest of the lattice. The emission spectrum is then shifted down in energy by the Stokes shift given by

$$E_a - E_b = 2\hbar\omega_{LO} .$$

In our $L$ x-ray emission spectrum of $a$-$SiO_2$ we observe an exciton peak centered at 105.3 eV. Thus we obtain Stokes shift of $0.36\pm0.15$ eV. This corresponds to a coupling constant $S$ of only $1.0\pm0.5$, indicating that incomplete phonon relaxation must be occurring in $a$-$SiO_2$.

## ACKNOWLEDGMENTS

The authors wish to thank Dr. B. Abeles of the Exxon Corporation for amorphous silicon dioxide samples and Professor W. B. Fowler for informative discussions. The authors acknowledge the help of C. Tarrio in obtaining and analyzing IES data and also R. D. Carson, P. Livins, D. Husk, P. Bruhwiler, and S. Velasquez for helpful discussions. This work was supported in part by the National Science Foundation under Grant No. DMR-85-15684.

[1] J. C. Phillips, in *Solid State Physics,* edited by H. Ehrenreich, F. Seitz, and D. Turnbull (Academic, New York, 1979), Vol. 37, p. 134.
[2] R. D. Carson, C. P. Frank, S. E. Schnatterly, and F. Zutavern, Rev. Sci. Instrum. **55**, 1973 (1984)
[3] P. C. Gibbons, J. J. Ritsko, and S. E. Schnatterly, Rev. Sci. Instrum. **46**, 1546 (1975).
[4] V. J. Nithianandam and S. E. Schnatterly, Phys. Rev. B **36**, 1159 (1987).
[5] J. R. Cuthill, in *X-Ray Spectroscopy,* edited by L. V. Azaraff (McGraw-Hill, New York, 1974), p. 164; G. A. Rooke, *ibid.*, p. 187.
[6] D. G. Hummer, Mem. R. Astr. Soc. **70**, 1 (1965).
[7] D. A. Stephenson and N. J. Binkowski, J. Non-Cryst. Solids **22**, 399 (1976).
[8] J. A. Tossell, D. J. Vaughn, and K. H. Johnson, Chem. Phys. Lett. **20**, 320 (1973).
[9] R. B. Laughlin, J. D. Joannopoulos, and D. J. Chadi, Phys. Rev. B **20**, 5528 (1979).
[10] S. T. Pantelides and W. A. Harrison, Phys. Rev. B **13**, 2667 (1976).
[11] R. N. Nucho and A. Madhukar, Phys. Rev. B **21**, 1576 (1980).
[12] R. P. Gupta, Phys. Rev. B **32**, 8278 (1985).
[13] K. L. Yip and W. B. Fowler, Phys. Rev. B **10**, 1391 (1974).
[14] K. L. Yip and W. B. Fowler, Phys. Rev. B **10**, 1400 (1974).
[15] W. B. Fowler, in *Structure and Bonding in Non-Crystalline Solids,* edited by G. W. Walrafen and A. G. Reversz (Plenum, New York, 1986), p. 157.
[16] I. A. Brytov and Yu. N. Romaschenko, Fiz. Tverd. Tela (Leningrad) **20**, 664 (1978) [Sov. Phys.—Solid State **20**, 384 (1978)].
[17] G. Weich and E. Z. Kurmaev, J. Phys. C **18**, 4393 (1985).
[18] G. B. Cherlov, S. P. Freidman, E. Z. Kurmaev, G. Weich, and V.A. Gubanov, J. Non-Cryst. Solids **94**, 276 (1987).
[19] H. Ibach and J. E. Rowe, Phys. Rev. B **10**, 710 (1974).
[20] A. M. Goodman, Phys. Rev. **144**, 588 (1966).
[21] E. O. Kane, Solid-State Electron. **28**, 3 (1985).
[22] W. Y. Ching, Phys. Rev. Lett. **46**, 607 (1981).
[23] F. C. Brown, R. Z. Bachrach, and M. Skibowski, Phys. Rev. B **15**, 4781 (1977).
[24] R. J. Elliot, Phys. Rev. **108**, 1384 (1957).
[25] A. Kotani and T. Toyozawa, in *Synchrotron Radiation,* edited by C. Kunz (Springer-Verlag, Berlin, 1979), p. 192.
[26] P. Livins (private communication).
[27] A. E. Meixner, P. M. Platzman, and M. Schlüter, in *The Physics of $SiO_2$,* edited by S. T. Pantelides (Pergamon, New York, 1978), p. 85.
[28] A. Koma and R. Ludeke, Phys. Rev. Lett. **35**, 105 (1975).
[29] J. Oliver, P. Faulconnier, and R. Poirier, in *The Physics of $SiO_2$,* Ref. 27, p. 89.
[30] R. B. Laughlin, Phys. Rev. B **22**, 3021 (1980).
[31] M. Rossinelli and M. A. Bosch, Phys. Rev. B **25**, 6482 (1982).
[32] Z. A. Weinberg, G. W. Rubloff, and E. Bassons, Phys. Rev. B **19**, 3107 (1979).
[33] H. R. Philipp, J. Phys. Chem. Solids **32**, 1935 (1971).
[34] D. L. Griscom, J. Non-Cryst. Solids **24**, 155 (1977).
[35] D. B. Fitchen, in *Physics of Color Centers,* edited by W. B. Fowler (Academic, New York, 1968), p. 299.
[36] F. J. Galeener and G. Lucovsky, Phys. Rev. Lett. **37**, 1474 (1976).
[37] D. A. Kleinman and W. G. Spitzer, Phys. Rev. **125**, 16 (1962).
[38] C. O. Ambladh, Phys. Rev. B **16**, 4343 (1977).